1/10th Scale Model Test of Inner Concrete Structure Composed of Concrete Filled Steel Bearing Wall

Hiroshi Akiyama
University of Tokyo, Tokyo, Japan
Hisashi Sekimoto, Mamoru Tanaka
Mitsubishi Heavy Industries, Ltd., Takasago, Japan
Kunio Inoue, Masaaki Fukihara, Yutaka Okuda
Mitsubishi Heavy Industries, Ltd., Kobe, Japan

1. Introduction

The inner concrete structure (IC) of a PWR type nuclear power plant is a double wall structure comprised of a primary shield wall, which supports and covers the center-located reactor vessel, and a secondary shield wall, which supports and covers steam generators, a pressurizer and a fuel transfer canal. The primary shield wall is a thick octagonal wall and the secondary wall surrounds the primary shield wall. These walls are made of a reinforced concrete structure (RC structure) in the existing nuclear power plants.

Recently, the demand for a shorter construction period and less site work for nuclear power plants has become greater and greater. It has made us investigate various new types of structures. Consequently we decided to study a concrete filled steel structure (SC structure) extensively.

On the premise that SC structure will be applied to IC of future nuclear power plants, this study was conducted using a 1/10 - scale model in order to obtain the necessary seismic design information, such as elastic and inelastic behavior, stiffness, ultimate strength, hysteresis characteristics and vibration characteristics under the horizontal seismic load.

2. Concept of SC Structure

2.1 Structural System and Construction Method

SC structure is a sandwich structure in which concrete lies between two surface steel plates. Namely RC structure would become SC structure if reinforcing bars in RC structure were taken out of the concrete and beaten into steel plates. Studs, shear bars and web plates are attached to the steel plate in order to obtain a composite effect of concrete and steel plates. Fig.1 shows the concept of SC structure.

SC structure is constructed by the process of (1) assembling of the steel unit by welding or bolting steel plates in the shop, (2) installation of the steel unit at the site, and (3) pouring of concrete into the steel unit, while RC structure is constructed by (1) fabrication of reinforcing bars (2) construction of forms and (3) pouring concrete.

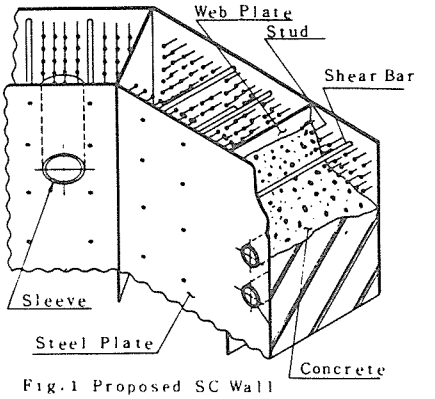

Fig.1 Proposed SC Wall

2.2 Advantages of SC structure

Advantages of SC structure are as follows.

(1) Shorter Construction Period
(2) Reduction of Site Work
(3) Simple Structure
(4) Cancellation of Embedded Plate
(5) Reduction of Temporary Work

3. Outline of Test

3.1 1/10 - Scale Model

The existing 1000MWe class plant was

selected and the RC structure of the primary and secondary shield walls was replaced by the SC structure. The model is on a scale of one to ten. The model was designed by the RC structure design method assuming that the steel plates are equivalent to the reinforcing bars. Photo.1 shows the test model and apparatus. Fig.2 shows the typical structure detail of SC structure wall (SC wall). As shown in Photo.1, the model consists of two parts. One is an SC structure part, which simulates the primary and secondary shield walls of the actual IC on a scale of one tenth, and the other is an RC structure part consisting of the base mat and the upper-and lower-loading slabs. SC walls are 110 mm thick and the surface steel plates are 1.4 mm thick. The material properties of concrete and steel plates used in the model are shown in Tables 1 and 2.

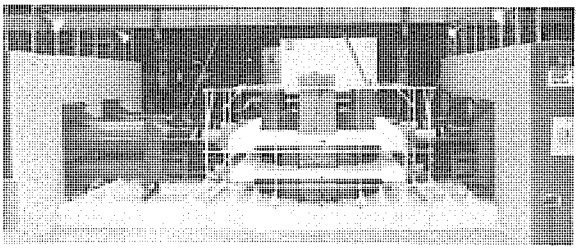

Photo.1 Test Model and Apparatus
(4.7m×4.25m×3.5mH)

Compressive Strength (MPa)	Tensile Strength (MPa)	Young's Modulus (KN/mm²)
17.4	1.5	16.8

Table 1 Material Properties of Concrete

	Size	Yield Stress (MPa)	Ultimate Strength (MPa)
Steel Plate	1.4^{t}mm	294	441
Shear Bar	2$^{\phi}$mm	569	667

Table 2 Material Properties of Structural Steel

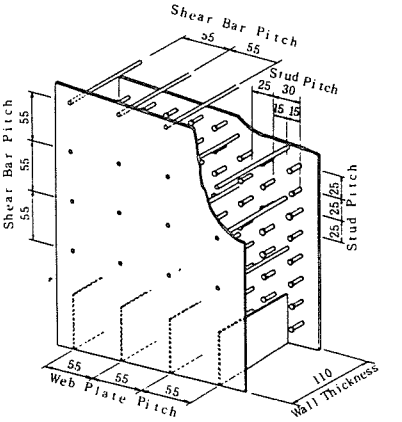

Fig.2 Typical SC Structure Detail

3.2 Test Procedure

The statical horizontal loading tests and the vibration tests were conducted alternately with the incremental increases of the horizontal load.

(1) Statical Horizontal Loading Test

The statical horizontal loading test was conducted in such a way that the base mat was fixed and the repetitive positive and negative loads were applied to the upper and lower loading slabs.

The loading direction was along the steam generator - reactor vessel - steam generator line. It was determined that the larger shear force was expected along this line in the seismic design. The ratio of the loads applied to upper and lower loading slabs was set at 1.0 (upper) and 0.385 (lower) in order to simulate the distribution of shear forces and bending moments assumed in the actual structure design.

(2) Vibration Test

The vibration test was conducted in such a way that the inertia type hydraulic shaker was fixed on the operating floor above the primary shield wall and the excitation force was applied in the same direction as that of the static horizontal loading test.

Sine sweep excitation was applied with the sweep frequency range between 20 - 200 Hz and 10 sec/Hz sweep velocity.

4. Test Results and Observations

4.1 Progress of Test

Fig.3 shows the relation of load to relative rotation angle obtained in this test. In Fig.3 the load (Q) means the total of the horizontal loads and the relative rotation angle (R) means the "value δ/H" obtained from dividing "the horizontal displacement of the upper loading slab δ" by "the distance from the upper edge of the base mat to the loading point of upper loading slab H".

Fig.4 shows the progress of the concrete crack and the steel plate yield. In Fig.4, the concrete crack occurrence was determined based on the load by

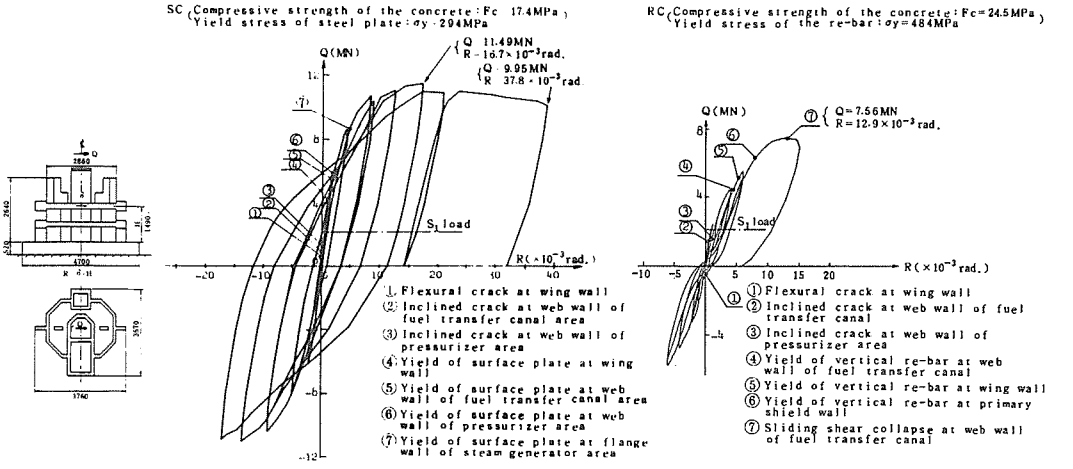

Fig.3 Load Relative Rotation Angle Relationship

which the measured steel plate strain reached the predetermined ultimate concrete tensile strain, while the steel plate yield was determined based on the load by which the measured steel plate strain reached the steel yield point.

The progress of the test is described as follows:

- In the 0.49 MN elastic cycle, no cracks were detected.
- In the 0.98 MN elastic cycle, concrete cracks occurred in the wing wall, the web wall of the fuel transfer canal area and the diagonal wall of the steam generator area. After this cycle, concrete cracks occurred as shown in Fig.4(a). Before the cycle of the relative rotation angle $R = 0.79 \times 10^{-3}$ rad. with the maximum load of 3.14 MN, almost all cracks had been already generated, however, in this cycle the relation of the load to relative rotation angle was still elastic.
- In the cycle of $R = 1 \times 10^{-3}$ rad. with the maximum load of 4.29 MN, the steel plate of the wing wall yielded. After this cycle, steel plate yielded as shown in Fig.4(b). And in the cycle of $R = 4 \times 10^{-3}$ rad. with the maximum load of 8.08 MN, elephant foot buckling of steel plate occurred in the lower part of the wing wall.
- In the cycle of $R = 12 \times 10^{-3}$ rad. with the maximum load of 10.95 MN, shear buckling of the steel plate occurred in the web wall of the fuel transfer canal area, the web wall of the pressurizer area and the diagonal wall of the steam generator area. In this cycle, elephant foot buckling of the steel plate also occurred at the bottom of the flange wall of the steam generator area. Because almost all steel plates had yielded before this cycle, the stiffness of the relation of the load to relative rotation angle, which had been decreasing gradually since the cycle of $R = 2 \times 10^{-3}$ rad., was decreased dramatically in this cycle. The maximum load of 11.49 MN was recorded in the cycle of $R = 17 \times 10^{-3}$ rad. and it turned out to be the maximum load in the test.
- In the last cycle, the steel plate of the first layer web wall of the fuel transfer canal area between the middle slab and the lower loading slab was broken off by the load of 3.92 MN as shown in Photo.2. However the load level was still being increased. After the relative rotation angle

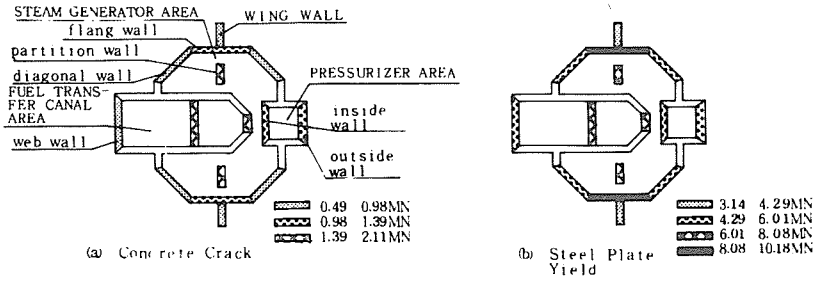

Fig.4 Progress of the Concrete Crack and Steel Plate Yield

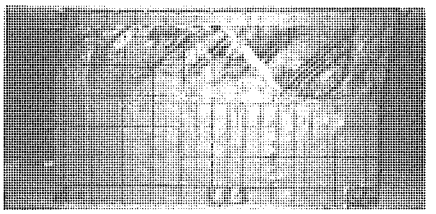

Photo.2 Final Collapse of Test Model

$R = 16.1 \times 10^{-3}$ rad. with the load of 10.79 MN, the displacement began to increase without load increase. After the relative rotation angle reached $R = 28.2 \times 10^{-3}$ rad., the load was decreased gradually. Finally the test was finished when the relative rotation angle $R = 37.8 \times 10^{-3}$ rad. with the load of 9.95 MN was recorded.

4.2 Model Characteristics

(1) Concrete Crack Occurrence Load

The comparison between the empirically obtained value and the calculated value concerning the concrete crack occurrence loads at the bottom of each wall is shown in Table 3. The calculated value in Table 3 was obtained from the following formula based on the results of the elastic analysis by finite element method (FEM) using a three dimensional shell element.

(Concrete crack occurrence load) = (Tensile strength of concrete)/(Principal tensile stress of concrete wall obtained from above calculation applied by unit load)

Location		Measured Qc, (MN)	Calculated Qc, (MN)	Qe/Qc
Wing Wall		0.68 ~ 0.78	0.85	0.80 ~ 0.92
Steam Generator Area	Flange wall	1.74 ~ 1.96	1.91	0.91 ~ 1.02
	Diagonal wall	1.74	1.54	1.13
	Partition wall	1.93	1.66	1.17
Fuel Transfer Canal Area	Web wall	1.16	1.80	0.64
Pressurizer Area	Web wall	1.95	2.36	0.83

Table 3 Comparison of Concrete Crack Occurrence Load (at the bottom of each wall)

Location		Measured Qe, (MN)	Calculated Qc, (MN)	Qe/Qc
Wing Wall		4.37	4.47	0.98
Steam Generator Area	Flange wall	8.53	9.58	0.89
	Diagonal wall	7.68	6.54	1.17
	Partition wall	7.67	7.70	1.00
Fuel Transfer Canal Area	Web wall	5.80	6.48	0.89
Pressurizer Area	Web wall	7.68	7.79	0.99

Table 4 Comparison of Steel Plate Yield Load (at the bottom of each wall)

Table 3 shows that the calculated result of the occurrence load at each wall and its occurrence order corresponds well to the experimental one.

(2) Steel Plate Yield Load

The comparison between the empirically obtained value and the calculated value of the steel plate yield load at the bottom of each wall is shown in Table 4. The calculated value of Table 4 are obtained by the following procedure based on result of the elastic FEM.

ⓐ Calculate forces in each member by FEM results.

ⓑ Assume that all tensile forces were sustained only by the steel plates.

ⓒ Assume that the compressive forces are sustained by the steel plates and concrete with the ratio of their stiffnesses.

ⓓ Calculate the stress components of steel plate from the member force obtained in ⓑ and ⓒ, and calculate the equivalent stress under the condition applied by unit load.

ⓔ (Yield load) = (Yield stress of steel)/(Equivalent stress obtained in ⓓ).

Table 4 shows that the calculated result corresponds very well to the experimental one.

The above mentioned yield load of each wall was considerably larger than S_1 load (the maximum design earthquake condition corresponding to US-SSE) of 2.11 MN. It is supposed that this is because the web plates contributions to the axial force and the concrete contributions to the shear forces parallel to the walls were not taken into account in the design of the model.

(3) Ultimate Strength

The test result showed that the ultimate strength was 11.49 MN and 5.5 times larger than the S_1 load. The ultimate strength Q_u of the test is calculated as 10.30 MN using the following ultimate shear strength formula.

$$Q_u = \tau_y A_s + 4.5 \sqrt{F_c} A_c$$

where; A_s : the cross section area of the surface steel plate
τ_y : the shear yield stress of the surface steel plate
A_c : the cross section area of concrete
F_c : the compressive strength of concrete
$4.5 \sqrt{F_c} A_c$: the ultimate shear strength of RC structure (FURUKAWA, 1987)

The quotient of the experimental value divided by the calculated value becomes 1.12, and it becomes obvious that the above formula can be applied to a complicated structure like the IC of a nuclear power plant.

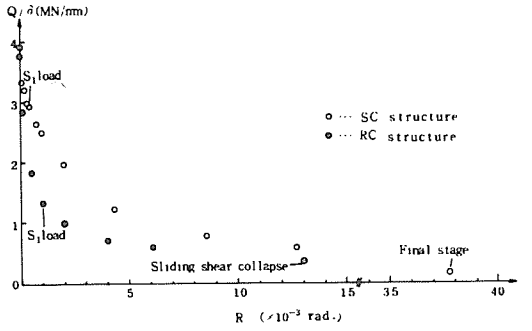

Fig.5 Stiffness Degradation

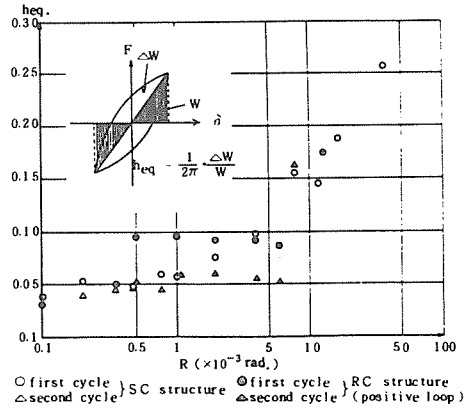

Fig.6 Equivalent Viscous Damping Factor

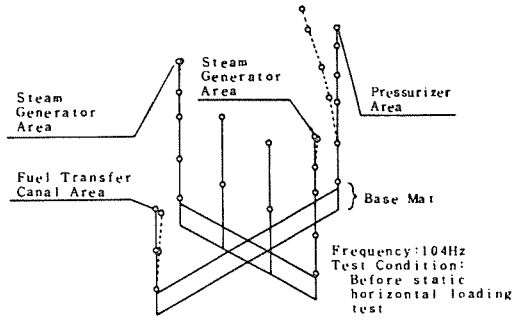

Fig.7 Vibration Mode

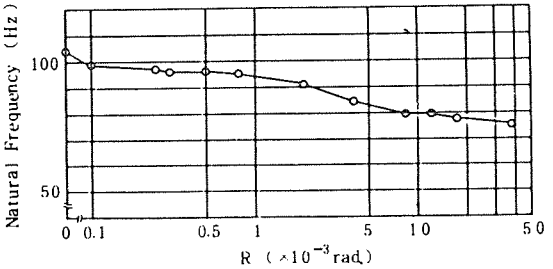

Fig.8 Natural Frequency vs. Experienced Relative Rotation Angle

(4) Stiffness Decrement

Fig.5 shows the stiffness decrement. In Fig.5, the vertical axis indicates secant modulus of stiffness and the horizontal axis indicates the relative rotation angle. As shown in Fig.5, the stiffness at S_1 load with $R = 0.48 \times 10^{-3}$ rad. decreased to 70% of the stiffness at elastic condition.

(5) Hysteresis Characteristics and Equivalent Viscous Damping Factor

As shown in Fig.3, the hysteresis characteristics of SC structure have a spindle-shape like steel structure and show a good behavior.

Fig.6 shows the equivalent viscous damping factor obtained from the loop of the load to relative rotation angle. In the tested SC structure, the equivalent viscous damping factor was about five percent before the steel yielded while it increased dramatically after the steel yielded. It is supposed that this is because the viscous damping governed the damping mechanism before the steel yielded while the hysteresis damping did so after the steel yielded.

(6) Vibration Characteristics

The fundamental vibration mode of IC is the mode in which the cantilever mode of the pressurizer area is distinguished as shown in Fig.7.

Fig.8 shows the relation between the experienced relative rotation angle and the natural frequency of the fundamental vibration mode of the IC shown in Fig.7. In Fig.8, the natural frequency decreased gradually from 104 Hz before static loading to 75.1 Hz after final static loading along the relative rotation hysteresis and no significant change in vibration mode was observed. It means that the stiffness distribution is almost constant up to the ultimate strength condition.

4.3 Comparison to IC of RC Structure

The IC of RC structure had been already studied using the same size scale model. (TAKEDA, 1983), (KATO, 1987) In order to compare the result of SC structure to that of RC structure, the results of RC structure are also added to Fig.3, 5 and 6. The following facts are derived from the comparison.

(1) The ultimate strength of SC structure is much higher than RC structure. The ultimate strength of SC structure was 11.49 MN while that of RC structure was 7.56 MN. This is because the ultimate strength of RC structure is evaluated by $Q_u = (4.5 \text{ to } 5.6)\sqrt{F_c}\, A_c$ including the reinforcing effect of the reinforcing bars while that of SC structure can be evaluated by $Q_u = \tau_y A_s + 4.5\sqrt{F_c}\, A_c$ in which the ultimate strength of steel plates can be added to that of concrete.

(2) RC structure lost its load carrying capacity rapidly because of the shear failure of the fuel transfer canal after it showed the maximum strength with the relative rotation angle $R = 12.9 \times 10^{-3}$ rad.. On the other hand, SC structure did not show deterioration even after the steel plate of the SC wall of the fuel transfer canal area was broken off. The final relative rotation angle recorded was $R = 37.8 \times 10^{-3}$ rad.. From this fact, it appears that SC structure is a very ductile structure.

(3) The stiffness decrease of SC structure is small compared with that of RC structure. For instance, at S_1 load, the stiffness decrease of RC structure is 65% while that of SC structure is only 30%.

(4) The equivalent viscous damping factor of the design load level is five percent in both RC and SC structures. In SC structure the equivalent viscous damping factor is almost constant at five percent before the steel yields and dramatically increases after that. On the contrary, in RC structure the equivalent viscous damping factor obtained from the second cycle loop is almost constant at a value of five percent before and after the reinforcing bar yields.

5. Conclusions

The repetitive positive and negative loading test, which simulated the earthquake excitation, and the vibration test were conducted using a 1/10 scale model of the IC of PWR type nuclear power plant adopting SC structure to its walls.

As a result of the test, SC structure shows superiority in ultimate strength and the ductile capability to RC structure and also shows well behaved hysteresis characteristics.

From now on, we would like to establish a rational design method for SC structure making the best use of its characteristics based on the reviews of this test and further studies.

References

FURUKAWA, S., TANAKA, H., IMOTO, K., YOSHIZAKI, S., INADA, Y., NANBA, H., EMORI, K. and SHIMIZU, A. (1987) Evaluation Method for Restoring Force Characteristics of R/C Shear Walls of Reactor Buildings (Part 1∿6). Abstracts of the Annual Congress of AIJ, pp. 289∿300.

KATO, M., WATANABE, Y., TAKEDA, T., YAMAGUCHI, T., ITO, M. and FURUYA, N. (1987). Horizontal Loading Tests on 1/10 Scale Model of Inner Concrete Structure for PWR-Type Nuclear Power Plant. 9th Intl. Conf. on Structural Mechanics in Reactor Technology, pp. 133∿142.

TAKEDA, T., YAMAGUCHI, T., ITO, M., FURUYA, N. and KIMURA, K. (1983). Horizontal Loading Tests and Vibration Tests on a 1/10 Scale Model of Inner Concrete Structure for PWR Type Nuclear Power Plant (PART I). Report of the Technical Research Institute Ohbayashi Corporation, No. 26, pp. 1∿9.